Mouse T-cell priming is enhanced by maturation-dependent stiffening of the dendritic cell cortex

Daniel Blumenthal[1], Vidhi Chandra[1], and Janis K. Burkhardt[1]*

[1]Department of Pathology and Laboratory Medicine, Children's Hospital of Philadelphia Research Institute and Perelman School of Medicine at the University of Pennsylvania, Philadelphia, PA, USA

*Correspondence:
Janis K. Burkhardt
Department of Pathology and Laboratory Medicine
Children's Hospital of Philadelphia Research Institute
3615 Civic Center Blvd, ARC 815D,
Philadelphia, PA 19104, USA
Tel: 267-426-5410
E-mail: jburkhar@pennmedicine.upenn.edu

Running Title: Modulation of T-cell activation by dendritic cell cortical stiffness

Key Words: actin, mechanotransduction, maturation, costimulation, signaling, cytoskeleton

ABSTRACT

T-cell activation by dendritic cells (DCs) depends on pushing and pulling forces exerted by the T-cell actin cytoskeleton. This process is enhanced by a series of changes in the DC, collectively termed maturation. Using atomic force microscopy, we show that during maturation, DC cortical stiffness is increased via a process that depends on actin polymerization. By manipulating the stiffness of T-cell substrates using stimulatory hydrogels or DCs expressing mutant cytoskeletal proteins, we show that increasing stiffness over the range observed during DC maturation enhances T-cell activation. Stiffness sensitivity is conserved in $CD4^+$ and $CD8^+$ T-cells, in both naïve and effector populations. Since increased stiffness lowers the agonist dose needed to activate naïve T cells, we conclude that mechanical cues function as co-stimulatory signals. Taken together, our data reveal that maturation-associated changes in the DC cytoskeleton alter its biophysical properties, creating a platform for enhanced mechanotransduction in interacting T-cells

INTRODUCTION

The initiation of an adaptive immune response requires priming of naïve T-cells by professional antigen presenting cells (APCs). This process requires multiple receptor-ligand interactions, which occur in concert at a specialized cell-cell contact site called the immunological synapse [1]. Through these interactions, APCs transmit a highly orchestrated series of signals that induce T-cell activation and direct differentiation of T-cell populations [2]. While the biochemical aspects of this process have been the subject of many studies, the contribution of mechanical cues is only now being uncovered.

Following initial T-cell receptor (TCR) engagement, T-cells apply pushing and pulling forces on interacting APCs [3-6]. These forces are essential for proper T-cell activation [7,8]. Moreover, force application is responsible, at least in part, for the ability of T-cells to rapidly discriminate between agonist and antagonist antigens [9,10]. While the mechanism by which force is translated into biochemical cues remains controversial [10-12], there is evidence that early tyrosine phosphorylation events downstream of TCR engagement occur at sites where applied force is maximal [6]. Interestingly, the amount of force a T-cell applies is directly affected by the stiffness of the stimulatory substrate [4,5]. Thus, it appears that force application is mechanically coupled to the T-cell's ability to sense stiffness (mechanosensing). In other cell types, substrate stiffness has been shown to affect a variety of cell functions including differentiation, migration, growth and survival [13-20]. Stiffness sensing in T cells has not been well studied, though there is some evidence that substrate stiffness affects both initial priming and effector functions [21-24]. Since the physiologically relevant substrate for T-cell priming is the surface of the interacting APC, one might predict that changes in cortical stiffness of the APC will profoundly influence T-cell priming. However, this prediction remained untested, and studies addressing the role of substrate stiffness in T-cell priming did not take into account the physiological stiffness of APCs.

Dendritic cells (DCs) are the dominant APCs that prime T-cells *in vivo* [25]. One of the hallmarks of DC biology is the process of maturation. Immature DCs are sentinels of the immune system, specialized for immune surveillance and antigen processing [26]. In response to infection or injury, inflammatory stimuli trigger signaling pathways that induce molecular reprogramming of the cell. The resulting mature DCs express high levels of surface ligands and cytokines needed for efficient T-cell priming [27]. The maturation process is tightly associated with remodeling of the DC actin cytoskeleton. This process underlies other maturation-associated changes such as

downregulation of endocytosis and increased migratory behavior [28,29]. In addition, cytoskeletal remodeling has a direct impact on the ability of mature DCs to prime T-cells [30,31]. Indeed, depolymerization of actin filaments perturbs the ability of mature peptide-pulsed DCs to activate T-cells, indicating that actin plays an important role on the DC side of the immunological synapse. We hypothesized that maturation-associated changes in the actin cytoskeleton modulate the stiffness of the DC cortex, and promote T-cell priming by providing physical resistance to the pushing and pulling forces exerted by the interacting T-cell.

In this work, we aimed to better understand the relationship between DC cortical stiffness and T-cell activation. We show that during maturation, DCs undergo a 2-3 fold increase in cortical stiffness, and that T-cell activation is sensitive to stiffness over the same range. Our results show that stiffness sensitivity is a general trait exhibited by most T-cell populations. Mechanosensing occurs through TCR engagement, and lowers the threshold signal required for T-cell activation. We conclude that stiffness serves as a novel biophysical costimulatory mechanism that functions in concert with canonical signaling cues to facilitate T-cell priming.

RESULTS

Dendritic cell stiffness increases upon maturation.

During maturation, DCs undergo a set of phenotypic changes that transform them into highly effective APCs [26]. We hypothesized that as part of this maturation process, DCs also modulate their cortical stiffness. To test this, we used atomic force microscopy (AFM) to directly measure cortical stiffness of immature and mature DCs. Murine bone marrow derived DCs (BMDCs) were prepared as described in Materials and Methods and cultured in the absence or presence of LPS to induce maturation. Cells were plated on Poly L-lysine (PLL) coated coverslips and allowed to spread for at least 4 hr prior to measurement of cortical stiffness by AFM micro-indentation. Because the population of LPS-treated cells was heterogeneous with respect to maturation markers, cells were labeled with fluorescent anti-CD86, and immature (CD86-negative) or mature (CD86 high) cells were selected for AFM measurements. As shown in Figure 1A, immature BMDCs were quite soft, with a mean Young's modulus of 2.2±0.7 kPa. Mature BMDCs were almost two-fold stiffer, with a Young's modulus of 3.5±1.0 kPa. Importantly, the stiffness of CD86-negative BMDCs within the LPS-treated population was the same as that of untreated, immature DCs. This demonstrates that the observed increase in stiffness is a property of DC maturation rather than an unrelated response to LPS treatment. Since BMDCs do not recapitulate all of the properties of classical, tissue resident DCs [32-34], we verified our results by measuring the stiffness of *ex-vivo* DCs purified from spleens of untreated or LPS-injected mice. Results were very similar; the stiffness of immature splenic DCs was nearly identical to that of immature BMDCs, and LPS treatment resulted in an increase in stiffness of almost 3-fold (Figure 1B). These results demonstrate that stiffness modulation is a *bona fide* trait of DC maturation. Moreover, they establish that the biologically relevant range of DC stiffness lies between 1 and 8 kPa.

The maturation-induced increase in stiffness is actin dependent and substrate independent.

One well-known feature of DC maturation is remodeling of the actin cytoskeleton. This process involves changes in the activation status of Rho GTPases and downstream actin regulatory proteins, and is known to downregulate antigen uptake and increase cell motility [28,29]. To ask if changes in actin cytoarchitecture also result in increased cortical stiffness, we treated immature and mature BMDCs with the actin-depolymerizing agents Cytochalasin-D or Latrunculin-B. Neither drug affected the stiffness of immature BMDCs, indicating that the basal level of stiffness depends on factors other than the actin cytoskeleton (Figure 1C). In contrast, both drugs induced a significant decrease in the stiffness of mature DCs, with Cytochalasin reducing their stiffness to

that of immature DCs. We conclude that the increased cortical stiffness observed upon DC maturation is another feature of actin cytoskeletal reprogramming.

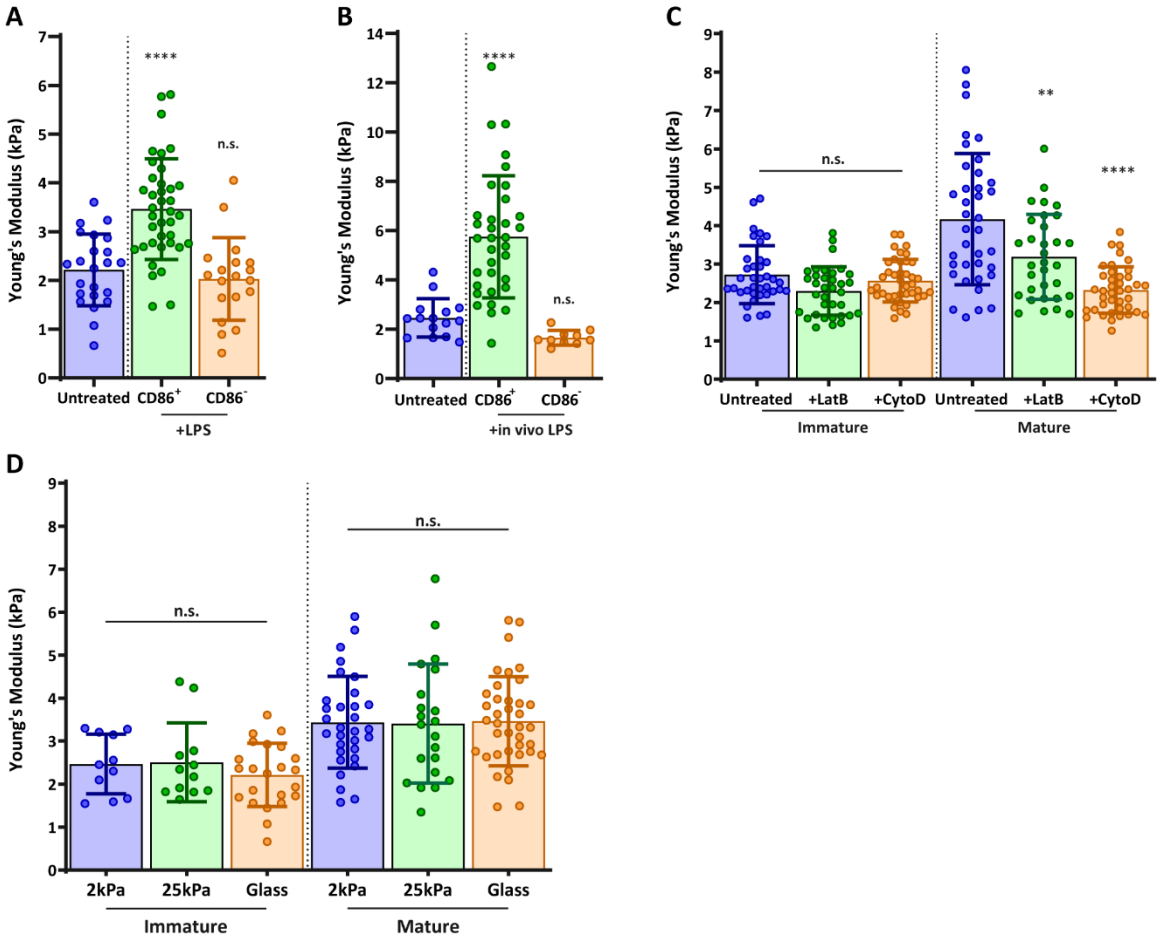

Figure 1. DC maturation induces an actin dependent increase in cortical stiffness.
(A) BMDCs were untreated or matured by treatment with LPS, and cortical stiffness was measured by AFM micro-indentation. Fluorescent anti-CD86 labeling was used to select immature (CD86-negative) or mature (CD86 high) cells. (B) E*x-vivo* DCs were purified from spleens of untreated mice or from mice injected with LPS 24 hr prior to harvesting the spleen. (C) Immature or LPS matured BMDCs either left untreated or treated with 10µM of the actin de-polymerizing agents Latrunculin-B or Cytochalasin-D prior to AFM measurements. (D) Immature or LPS matured BMDCs were plated on substrates of different stiffness prior to AFM measurements. Each data point represents an average of two stiffness measurements at different locations around a single cell nucleus. Data are pooled from 3 experiments (A) or 2 experiments (B-D). Error bars denote standard deviation. n.s non-significant, **$p<0.01$, ****$p<0.0001$ calculated by an unpaired one-way ANOVA, post-hoc Tukey corrected test.

Some cell types regulate their stiffness in response to the stiffness of their substrate[13,35]. To test whether DCs exhibit this behavior, immature and mature BMDCs were plated on PLL-coated substrates of different compliances (hydrogels of 2 or 25 kPa, or glass surfaces in the GPa range)

and allowed to spread on the surface for at least 4 hr prior to AFM measurement. No apparent difference in cell spreading or morphology could be noted on the different PLL-coated hydrogels (data not shown). Hydrogel compliance was verified by measuring the elastic modulus of the surface in areas devoid of cells (Figure 1 - Figure Supplement 1). As shown in Figure 1D, substrate compliance had no effect on cortical stiffness of either immature or mature BMDCs. In control studies, we could readily detect substrate-dependent changes in stiffness of normal fibroblast cells (not shown). Thus, we conclude that DCs maintain a specific cortical stiffness, which is characteristic of their maturation state.

Stiffness increases over the physiological range lower the threshold for T-cell activation.

Our findings raise the possibility that changes in DC cortical stiffness, like other maturation-induced changes, enhance the ability of these cells to prime a T-cell response. Two previous studies showed that T-cell activation is dependent on the stiffness of stimulatory surfaces[21,22], but results were conflicting. Moreover, neither study was performed within the stiffness range that we now show is relevant for DCs. Thus, we tested T-cell responses on hydrogels with a stiffness range spanning that of immature and mature DCs (1 – 25 kPa). Hydrogel compliance was verified by measuring the elastic modulus of the surfaces directly and stiffness values were found to be similar to those reported by the manufacturer (Figure 2 - Figure Supplement 1). Surfaces were coated with varying doses of anti-CD3ε together with a constant dose of anti-CD28, and used to stimulate *ex-vivo* murine $CD4^+$ or $CD8^+$ T-cells. Plastic surfaces, which are commonly used for stimulation with surface-bound ligands, were included as a familiar reference point. As one measure of T-cell activation, proliferation was assessed based on CFSE dilution after 72 hr. For both $CD4^+$ and $CD8^+$ T-cells (Figure 2 A,B and C,D respectively), T-cell proliferation was enhanced by increased substrate stiffness. This was particularly evident at low doses of anti-CD3ε (0.1-0.3ug/ml). Notably, the effect of substrate stiffness on T-cell activation was not binary. Instead, each individual substrate stiffness showed an anti-CD3ε dose response, and the threshold dose required to induce robust proliferation shifted as a function of substrate stiffness. Importantly, over the stiffness range associated with DC maturation (1-8kPa), the dose of TCR signal needed to induce proliferation was shifted by more than 10-fold. Control studies showed that the stimulatory antibodies bound similarly to the different hydrogels (Figure 2 – Figure Supplement 2), ruling out the possibility that differences in T-cell activation are due to differential antibody binding.

The studies above were performed using anti-CD3, which has a very high binding affinity, and which may not appropriately model mechanobiology of TCR αβ engagement. Thus, we next asked if the observed stiffness sensitivity is conserved when T cells are stimulated with pMHC complexes. Surfaces were coated with varying doses of MHC-II covalently bound to $OVA_{(323-339)}$ peptide (pMHC-II), together with a constant dose of anti-CD28, and used to stimulate *ex-vivo,* OVA specific, OT-II TCR transgenic $CD4^+$ T-cells. Strikingly, OT-II T cells showed the same stiffness response observed for $CD4^+$ and $CD8^+$ T-cells stimulated with anti-CD3ε antibody (Figure 2E,F).

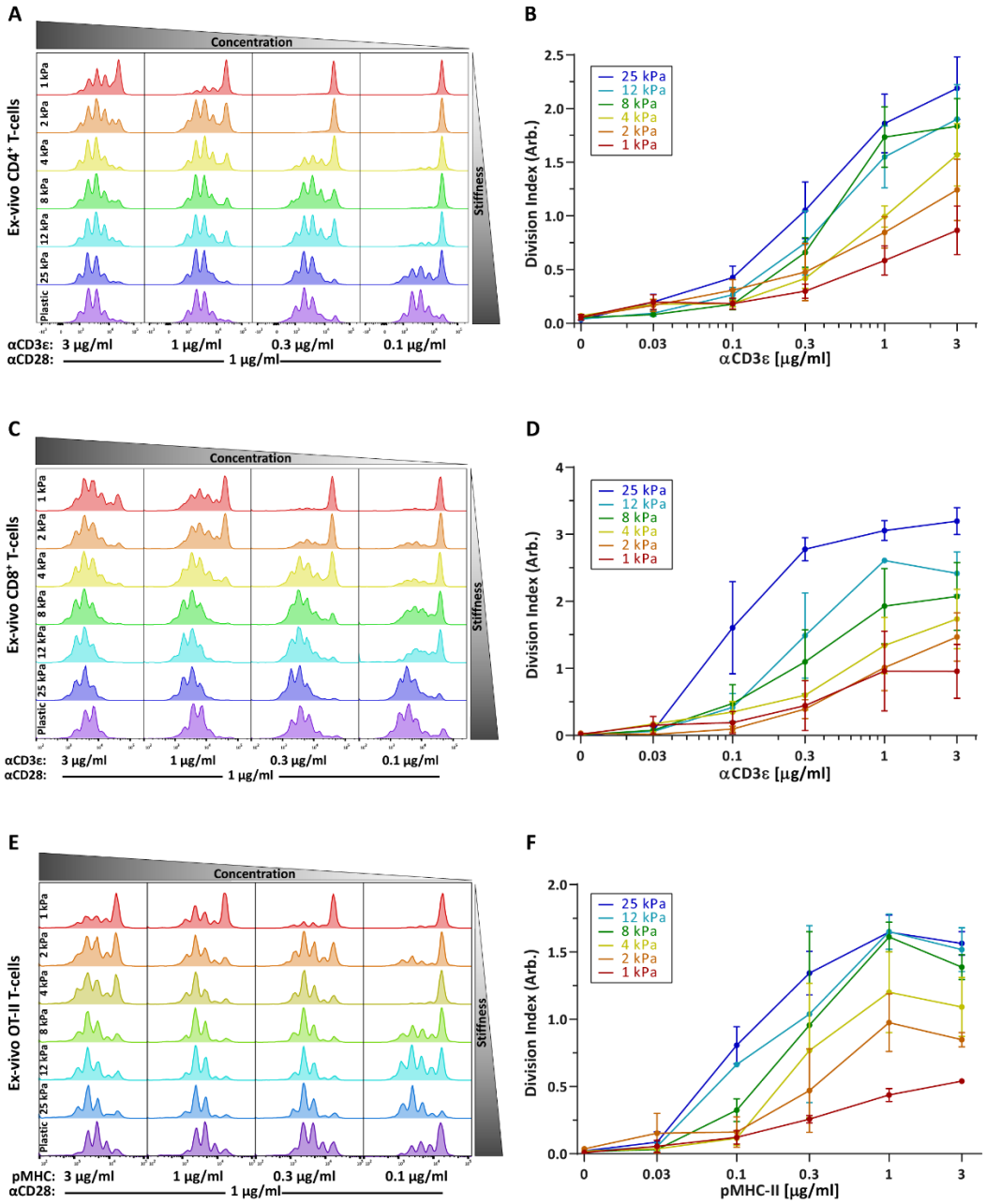

Figure 2. Proliferation of ex vivo CD4+ and CD8+ T cells is stiffness dependent.
Murine T-cells were purified from lymph nodes and spleen and activated on stimulatory acrylamide hydrogel surfaces with a stiffness range of 1 – 25 kPa. (A-B) *Ex-vivo* $CD4^+$ T-cells were activated on hydrogels coated with the indicated concentrations of anti-CD3ε, together with 1 µg/ml anti-CD28, and T-cell responses were assessed. (A) Proliferation of $CD4^+$ T-cells was measured by CFSE dilution at 72 hr post activation. (B) Division index values extracted from 5 independent experiments. (C-D) *Ex-vivo* $CD8^+$ T-cells were activated on hydrogels coated with the indicated concentrations of anti-CD3ε, together with 1 µg/ml anti-CD28, and T-cell responses were assessed. (C) Proliferation of $CD8^+$ T-cells was measured by CFSE dilution at 72 hr post activation. (D) Division index values extracted from 3 independent experiments. (E-F) *Ex-vivo* OT-II $CD4^+$ T-cells were activated on hydrogels coated with the indicated concentrations of pMHC-II, together with 1 µg/ml anti-CD28, and T-cell responses were assessed. (C) Proliferation of $CD4^+$ T-cells was measured by CFSE dilution at 72 hr post activation. (D) Division index values extracted from 2 independent experiments.

As an independent means of assessing T-cell activation, we measured IL-2 secretion by *ex vivo* $CD8^+$ T-cells after 18 hr. As shown in Figure 3A, increased substrate stiffness decreased the dose of anti-CD3ε needed to induce IL-2 secretion. A similar stiffness dependence for IL-2 production was observed for $CD4^+$ T-cells (Figure 3B). As with proliferation, IL-2 production by both $CD4^+$ and $CD8^+$ T-cells was significantly enhanced by increases in stiffness over the range observed for DCs (1-8kPa). For both T-cell types, we observed a further increase in IL-2 production and proliferation on the 25 kPa and plastic substrates, though the physiological relevance of this is not clear. Since the threshold stimuli (stiffness and dose of anti-CD3ε) required to induce significant IL-2 production and proliferation were very similar, we reasoned that the two might be causally related (i.e. the threshold for proliferation might be driven by the need for IL-2 secretion). To test this, we asked if the addition of exogenous IL-2 would rescue the proliferation of $CD4^+$ T-cells stimulated on soft surfaces. As shown in Figure 3C, exogenous IL-2 did not rescue proliferation. We conclude that substrate stiffness affects the signaling threshold for IL-2 production as well as other, IL-2 independent events needed for efficient T-cell proliferation. Taken together, our findings point to a mechanism in which stiffer substrates have a sensitizing effect on T-cells, similar to that of classical co-stimulatory molecules such as CD28 [36].

<u>Cytotoxic T-cells also exhibit stiffness dependence.</u>

Whereas naïve T-cells are activated by DCs, effector T-cells interact with many cell types. In particular, cytotoxic $CD8^+$ T-cells (CTLs) must respond to a variety of possible target cells, which may differ widely with respect to stiffness. We therefore reasoned that CTL effectors might be stiffness independent. To test this, *ex-vivo* $CD8^+$ T-cells were activated on plastic surfaces and

grown in the presence of IL-2 to produce mature CTLs. To induce and detect release of cytolytic granules, CTLs were re-stimulated on hydrogels coated with a range of anti-CD3ε concentrations in the presence of fluorescent anti-CD107a antibody, and analyzed by flow cytometry. Somewhat surprisingly, we found that CTL degranulation is stiffness dependent (Figure 3D). Interestingly, however, changes in substrate stiffness within the range we measured for most DCs (1-4kPa) had little or no impact on degranulation. Increased degranulation was first detected at 8-12kPa, and was most pronounced on very stiff surfaces (25 kPa and plastic). This may be important for effector function *in vivo*, where target cells in inflamed tissues may reach this stiffness range.

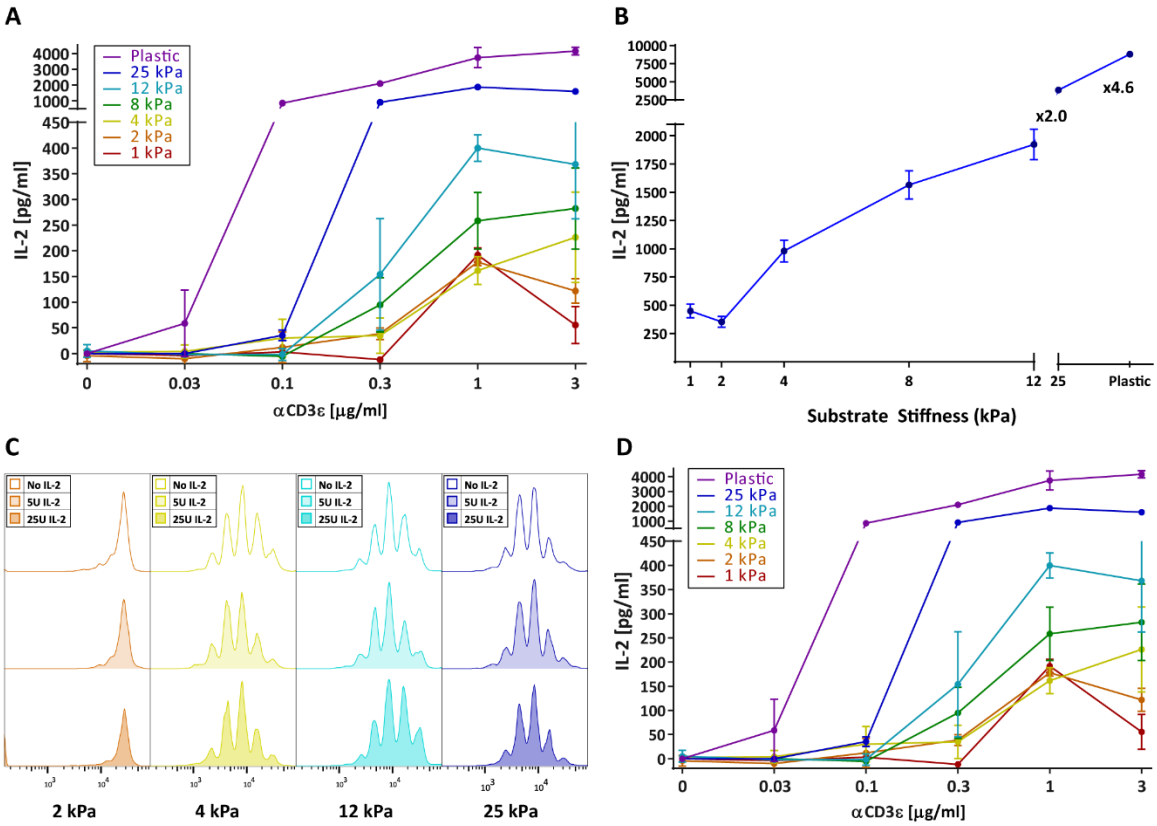

Figure 3. IL-2 production and CTL degranulation is stiffness dependent

(A-C) Murine T-cells were purified from lymph nodes and spleen and activated on stimulatory acrylamide hydrogel surfaces with a stiffness range of 1 – 25 kPa. (A) $CD8^+$ T-cells were activated on a range of anti-CD3ε concentrations together with 1 μg/ml anti-CD28 and IL-2 secretion was measured by ELISA at 18 hr post activation. Data represent means +/- StDev from 9 replicate samples from 2 experiments. (B) $CD4^+$ T-cells were activated on 1 μg/ml anti-CD3ε and anti-CD28 and IL-2 secretion was measured by ELISA at 18 hr post activation. Data represent means +/- StDev from 6 replicate samples from one representative experiment. (C) Proliferation of *ex-vivo* $CD4^+$ T-cells activated in the presence of exogenous IL-2 (5 or 25U/ml), was measured by CFSE dilution at 72 hr post activation. (D) Cytotoxic $CD8^+$ T-cells on days 8 or 9 of culture were restimulated on hydrogel surfaces with a range of anti-CD3ε concentrations. Degranulation was measured based on surface exposure of CD107a.

T-cells sense stiffness through the T-cell receptor and not CD28.

Mechanosensing usually involves intracellular forces exerted on cell surface receptors bound to surface-attached ligands. Since TCR triggering is a force-dependent process [3-7], we reasoned that stiffness sensing might be TCR dependent. To ask if the process involves the TCR, the co-stimulatory molecule CD28, or both, we used a strategy developed by Judokusomo et al. [21]. *Ex vivo* $CD4^+$ T-cells were activated with hydrogels of different stiffness coated with one activating antibody, while the other antibody was coated onto stiff, 6 µm polystyrene beads and presented in *trans*. To explore the costimulatory dose response, the bead-bound antibodies were titrated from bead saturation to three orders of magnitude lower. Proliferation was measured by CFSE dilution and is presented as division index for the sake of simplicity. In each case, the response of T-cells stimulated in *cis* with hydrogels coated with both anti-CD3ε and anti-CD28 is plotted as a dashed line to facilitate comparison. When anti-CD28 was coated on the hydrogels, T-cell activation was the same across the entire stiffness range for any given dose of anti-CD3ε (Figure 4A). Conversely, when anti-CD3ε was coated on the hydrogels, T-cells exhibited a stiffness-dependent response (Figure 4B). A stiffness-dependent response was observed at all doses of anti-CD28, but at higher doses, where T-cell proliferation was robust, there was a sharp increase in proliferation over the stiffness range observed for DCs (1-8 kPa). Note that the stiffness response to anti-CD3 and anti-CD28 differs somewhat depending on whether the two signals are delivered in cis or trans, possibly reflecting the involvement of mechanical crosstalk between the two molecules [6,37,38].

Interestingly, we found that very stiff substrates (≥25 kPa) can induce proliferation even in the absence of any classical CD28 co-stimulation (Figure 4B and Figure Supplement 1). In fact, activation on plastic surfaces eliminates the requirement for CD28 altogether, suggesting that under some extreme (non-physiological) conditions, stiffness signals alone are sufficient to costimulate T-cell activation. Taken together, these findings demonstrate that the TCR, and not CD28, is a T-cell mechanosensor. This conclusion supports and extends previous work addressing this question [21], by showing that the TCR senses substrate stiffness within the range relevant for DCs.

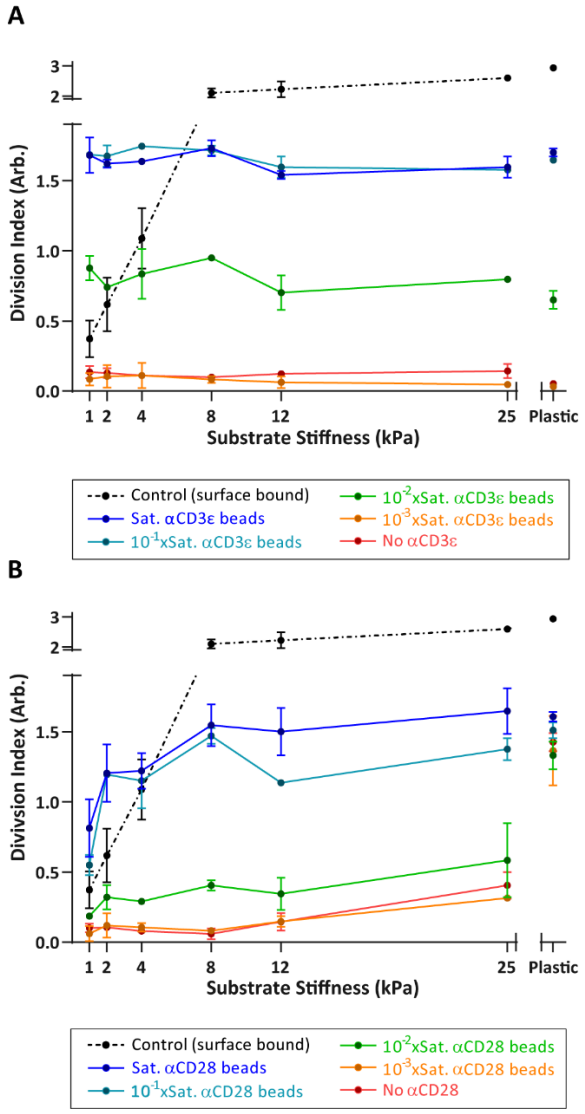

Figure 4. T-cells sense stiffness through the TCR and not CD28

Ex-vivo CD4⁺ T-cells were activated on hydrogel surfaces of different stiffness coated with one activating antibody (anti-CD3ε or anti-CD28) and stiff, 6 µm polystyrene beads coated with the other (trans stimulation). Bead-bound antibodies were titrated from bead saturation to three orders of magnitude lower. Proliferation was measured by CFSE dilution and the fraction of divided cells was used to facilitate comparison. Dashed line represents a control experiment where hydrogels were coated with both stimulatory antibodies (cis stimulation). (A) Hydrogel surfaces were coated with anti-CD28 and beads were coated with anti-CD3ε. (B) Hydrogel surfaces were coated with anti-CD3ε and beads were coated with anti-CD28. Data represent means +/- StDev for duplicate samples from one representative experiment (N=3 experiments).

DC cortical stiffness is primarily controlled by actin polymerization

To better understand the relationship between DC cortical stiffness and T-cell activation, we sought to identify the molecular mechanisms controlling DC cortical stiffness. Several actin regulatory mechanisms are known to change during DC maturation. In particular, mature DCs upregulate the actin bundling protein fascin[39], they show activation of myosin-dependent processes [40], and they undergo changes in the activation and localization of Rho-GTPases, which in turn regulate actin polymerization via the Arp2/3 complex and formins [28,29,41]. To ask how each of these pathways influences cortical stiffness, we used small molecule inhibitors and DCs from relevant knockout mice. Note that to facilitate comparison between experiments, control immature and mature DCs were tested in each experiment, and results were normalized based on values for mature DCs. First, we tested the role of fascin, which is known to generate very stiff

actin bundles *in vitro*[42]. Surprisingly, the stiffness of BMDCs from fascin-KO mice was indistinguishable from that of WT BMDCs both before and after LPS-induced maturation (Figure 5A). Next, we tested the contribution of myosin contractility, which is known to control stiffness and membrane tension in other cell types [43]. As shown in Figure 5B, treating mature BMDCs with the myosin II inhibitor blebbistatin reduced stiffness by a small, albeit statistically significant amount. Similar results were obtained with the Rho-kinase (ROCK) inhibitor Y27623, which indirectly inhibits myosin function. Thus, we conclude that myosin contractility plays a relatively minor role in regulating DC cortical stiffness.

We next tested the possibility that cortical stiffness is modulated by actin polymerization. Broadly speaking, actin polymerization is induced by two sets of proteins: formins generate linear actin filaments, while activators of the Arp2/3 complex produce branched actin structures. As shown in Figure 5B, treatment of DCs with the pan-formin inhibitor SMIFH2 significantly reduced the cortical stiffness of mature DCs. A similar reduction in cortical stiffness was observed after inhibition of Arp2/3-mediated branched actin polymerization by CK666. DCs express multiple activators of Arp2/3 complex, of which two have been implicated in maturation-associated changes in actin architecture: Hematopoietic Lineage Cell-Specific Protein 1 (HS1), the hematopoietic homologue of cortactin [44], and WASp, the protein defective in Wiskott-Aldrich syndrome [45-47]. To individually assess the role of these two proteins, we used BMDCs cultured from HS1 and WASp knockout mice. As shown in Figure 5A, loss of HS1 had no impact on cortical stiffness of either immature or mature BMDCs. In contrast, mature WASp knockout BMDCs were significantly less stiff than WT controls. This difference mirrors that seen after inhibition of Arp2/3 complex by CK666, suggesting that WASp is the primary activator of Arp2/3 complex-dependent changes in cortical stiffness. The defect in WASp knockout DCs was observed only after maturation; immature WASp knockout DCs did not differ in stiffness from WT controls. This is consistent with our finding that the stiffness of immature DCs is unaffected by actin depolymerizing agents. Taken together, these results show that activation of formin and WASp-dependent actin polymerization pathways, and to a lesser extent increased myosin contractility, all contribute to the increased cortical stiffness of mature DCs.

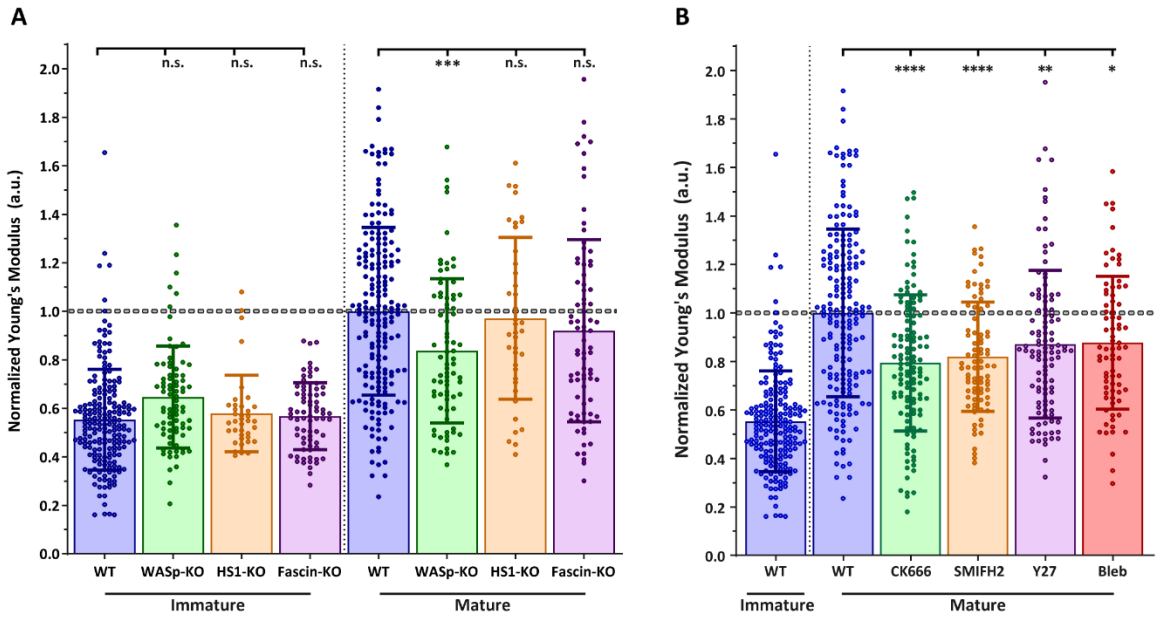

Figure 5. Effects of actin regulatory proteins on DC cortical stiffness

Murine BMDCs from WT mice or mice lacking key actin-associated proteins were untreated or matured by treatment with LPS. Cortical stiffness was measured by AFM micro-indentation. To facilitate comparison between experiments, results were normalized to values of mature WT BMDCs in each experiment. (A) Cortical stiffness of BMDCs from mice lacking important actin modulating proteins. (B) Cortical stiffness of WT BMDCs treated with cytoskeletal inhibitors. CK666 (100 µM) was used to inhibit branched actin polymerization. SMIFH2 (10 µm) was used to inhibit linear actin polymerization. Acto-myosin contractility was inhibited directly with Blebbstatin (50 µM) or indirectly with the Rho-kinase inhibitor Y27623 (25 µM). All drugs had no effect on immature BMDCs (data not shown). Data points for untreated WT BMDCs (both immature and mature) were pooled from all experiments as a reference. The dashed line represents the average stiffness of untreated mature WT BMDCs from all experiments. Each data point represents an average of two stiffness measurements at different locations around a single cell nucleus. Error bars denote standard deviation. Data are pooled from 2-3 independent experiments. n.s non-significant, *$p<0.05$, **$p<0.01$, ***$p<0.001$, ****$p<0.0001$ calculated by an unpaired one-way ANOVA, with post-hoc Tukey correction.

<u>The increased stiffness of mature DCs enhances their ability to prime T-cells</u>

Our hydrogels assays showed that T-cell activation is enhanced by changes in stiffness over the range observed during DC maturation. This finding strongly suggests that cortical stiffness is a biophysical mechanism by which DCs control T-cell activation. To test this directly, we sought conditions under which we could manipulate the stiffness of mature DCs. We took advantage of our finding that mature WASp knockout BMDCs are approximately 20% softer than WT controls (Figure 5A; Figure 6A shows absolute values). To generate DCs that are stiffer than WT-cells, we

transduced BMDCs with a constituently active form of WASp (I294T, CA-WASp [48]). As shown in Figure 6A, this increases cortical stiffness of mature BMDCs by approximately 20% relative to WT-cells. We then used this panel of DCs to test whether cortical stiffness affects the ability of mature DCs to prime a T-cell response. WT BMDCs and either WASp-KO or CA-WASp-transduced BMDCs were pulsed with increasing concentrations of $OVA_{323-339}$ peptide and co-cultured with OT-II $CD4^+$ T-cells. T-cell proliferation was measured by CFSE dilution. Figures 6B,D,F show that WASp-KO BMDCs do not prime T-cells to the same extent as WT BMDCs at low OVA concentrations. Higher concentrations of OVA rescued this defect, showing that loss of WASp shifts the dose of peptide needed rather than affecting T-cell priming *per se.* BMDCs expressing CA-WASp, however, failed to prime T-cells more efficiently than WT BMDCs (Figure 6C,E,G). These results relating WASp-dependent DC stiffness to T-cell priming can best be understood in the context of T-cell responses to hydrogels (Figure 2). T-cell proliferation is significantly enhanced by increases in hydrogel stiffness in the range of 2-4kPa, which spans the difference between WASp-KO and WT DCs. In contrast, increases in stiffness above 4kPa have significantly less pronounced effects on T-cell priming. In the hydrogel system, even an increase from 4 to 8 kPa has only modest effects. Thus, T-cells would not be expected to show increased activation on DCs expressing CA-WASp, which only increases stiffness to about 5 kPa. Data from T cells responding to hydrogels and genetically manipulated DCs are plotted together, to facilitate this comparison (Figure 6 – Figure Supplement 1). Although we tried several strategies aimed at generating DCs a cortical stiffness of 8kPa or higher, we were unable to do so. Thus, we have been unable to directly test the effects of increasing DC stiffness above the range we observe after maturation with LPS. Within the range that we have been able to test, our results show that T-cells respond to the stiffness of DCs much as they do to artificial stimulatory surfaces, supporting the idea that maturation-induced increases in DC stiffness contribute to the enhanced ability of mature DCs to prime a T-cell response.

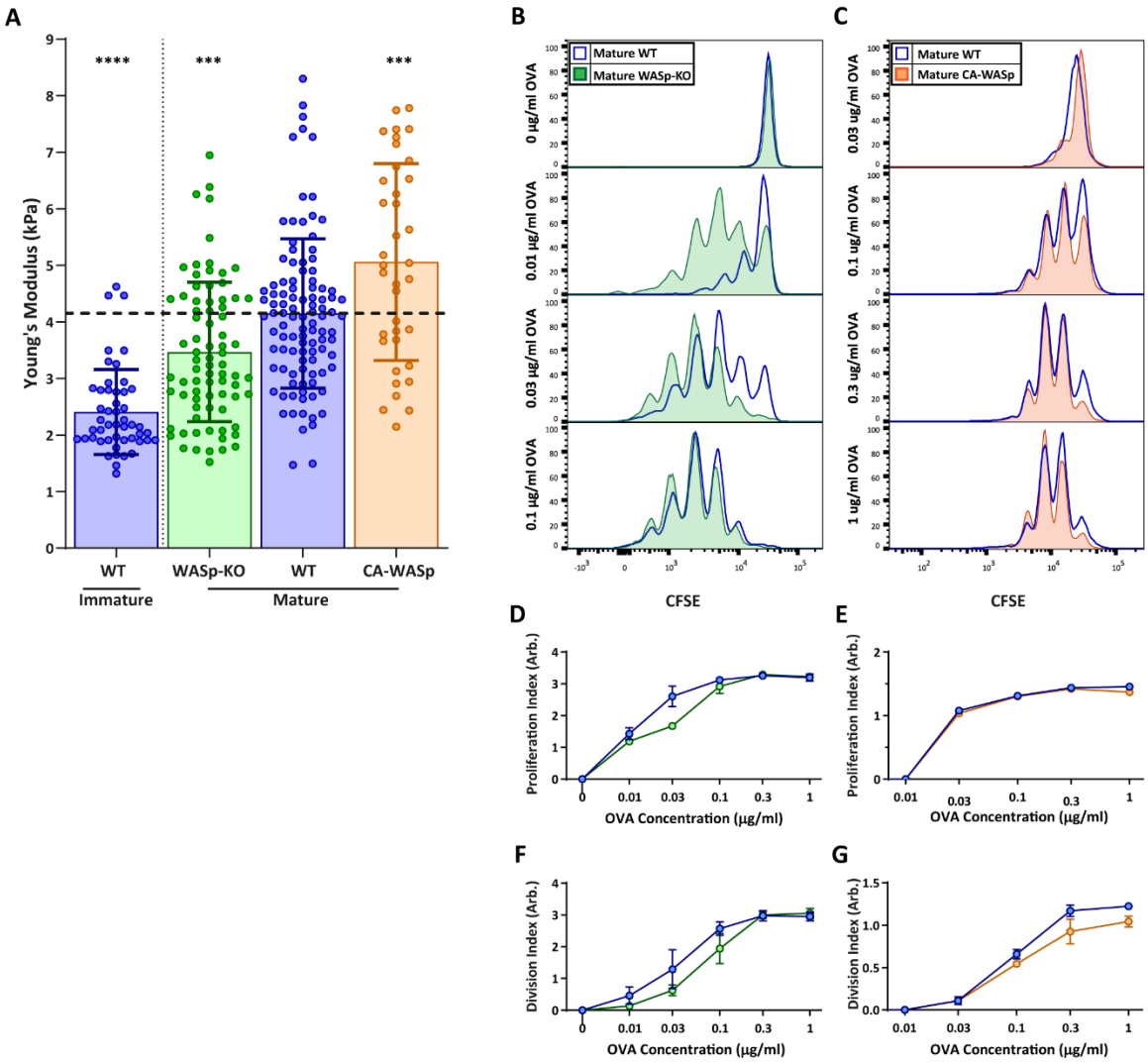

Figure 6. DC cortical stiffness acts as a costimulatory signal for T-cell activation

WT, WASp-KO BMDCs, or WT BMDCs transduced with constituently active form of WASp (CA-WASp) were untreated or matured by treatment with LPS. (A) Cortical stiffness was measured by AFM micro-indentation. Each data point represents an average of two stiffness measurements at different locations around a single cell nucleus. Error bars denote standard deviation. ***p<0.001, ****p<0.0001 calculated by an unpaired one-way ANOVA, comparing mature WT with all other treatments, with post-hoc Tukey correction. (B,C) LPS-matured BMDCs were pulsed with a range of $OVA_{323-339}$ peptide concentrations and co-cultured with *ex-vivo* OT-II $CD4^+$ T-cells for 72 hrs. Proliferation was measured by CFSE dilution. (D,E) Proliferation index pooled from two independent experiments. (F-G) Division index values pooled from two independent experiments. Error bars represent StDev. (B) Comparison of T-cell activation by WT or WASp-KO mature DCs, aggregate quantification of proliferation and division indices are given in D and F respectively. (C) Comparison of T-cell activation by WT or CA-WASp mature DCs, aggregate quantification of proliferation and division indices are given in E and G respectively.

DISCUSSION

Recent work from several labs clearly shows that T-cell activation involves mechanical cues. We have previously shown that the DC cytoskeleton constrains the mobility of stimulatory ligands on the DC surface, thus enhancing T-cell activation by opposing the forces exerted by the T-cell on the corresponding receptors [30]. In the current study, we elucidate a second mechanism whereby the DC cytoskeleton enhances T-cell activation. We show that actin remodeling during DC maturation increases the cortical stiffness of DCs by 2-3 fold, and that T-cell activation is enhanced by increases in stiffness over the same range. Importantly, increased stiffness lowers the threshold dose of TCR ligand needed for T-cell activation, as expected if substrate stiffness serves as a costimulatory signal. Stiffness sensitivity was conserved in naïve $CD4^+$ and $CD8^+$ T-cells, as well as in effector $CD8^+$ T-cells. Moreover, we observed a similar response to stimulation through CD3 and pMHC-II. Taken together, these results indicate that stiffness sensitivity is a general feature of T-cell biology.

Modulation of actin architecture has long been appreciated as an essential feature of DC maturation. Changes in the DC actin cytoskeleton facilitate the transition from highly endocytic tissue-resident cells to migratory cells specialized for antigen presentation [27,41]. Our findings reveal a new facet of this process. We show that immature DCs are very soft, and that upon maturation, their cortical stiffness is increased by 2-3 fold. This is true for both cultured BMDCs treated with LPS *in vitro*, as well and splenic DCs harvested from LPS-treated mice. A similar trend was reported by Bufi et al for human monocyte-derived DCs[49], although that study reported lower absolute Young's modulus values. While we used AFM indentation, Bufi et al. used microplate rheology. Since different methods for measuring cell mechanical properties produce absolute Young's modulus values that can vary by as much as 100 fold [50], it seems likely that the apparent discrepancy in absolute values stems from technical differences between the two studies. Nevertheless, it is clear from both studies that the stiffness of the DC cortex is modulated during maturation.

We show that the increase in DC stiffness depends on changes in actin architecture; whereas depolymerization of actin filaments does not affect the stiffness of immature DCs, it does perturb the increase associated with maturation. In particular, this increase is sensitive to inhibitors of actin polymerizing molecules. While it remains to be determined exactly which actin regulatory pathways control cortical stiffness in mature DCs, our data show that both

Arp2/3 complex and formins are involved. Moreover, we find that DCs lacking the Arp2/3 activator WASp are abnormally soft. In keeping with these findings, DC maturation is known to induce changes in the activation state and localization of Rho family GTPases, especially Cdc42, a molecule that can activate both WASp and formins [28,29,51]. Since the overall levels of active Cdc42 are diminished during DC activation, it seems likely that the observed increase in cortical stiffness results from relocalization of the active pool.

Importantly, we show that DC cortical stiffness is a cell intrinsic property that is unaffected by substrate stiffness. In this respect, DCs are different from other cell types that adapt their stiffness to differences in substrate compliance [13,35]. The ability of DCs to maintain constant stiffness despite changing environmental cues is reminiscent of previous work showing that DCs rapidly change their method of locomotion in order to maintain consistent migration speed and shape while crossing over different surfaces [52]. This behavior has been proposed to allow DCs to pass through tissues with widely different mechanical properties. In the same way, we propose that the ability of DCs to regulate cortical stiffness as a function of maturation state in spite of environmental cues reflects the importance of this property for priming an appropriate T-cell response.

A central finding of this paper is that T-cell priming is sensitive to changes in stiffness over the physiologically relevant range, as defined by immature and mature DCs (1 – 8 kPa). Importantly, by using a matrix of different hydrogels and anti-CD3ε concentrations, we found that stimulatory substrates with lower stiffness required higher concentrations of anti-CD3ε to achieve T-cell activation. Similarly, when compared to WT DCs, softer WASp knockout DCs required higher concentrations of OVA peptide to induce the same level of proliferation. Therefore, we propose that stiffness is a novel costimulatory mechanism that, similar to CD28 [36], lowers the threshold for T-cell activation.

Since increasing cortical stiffness is part of DC maturation, stiffness may present a new signaling mechanism by which DCs not only modulate activation but also control T-cell fate and differentiation. Bufi et al. showed previously that human monocyte-derived DCs responding to different maturation signals vary in their stiffness [49]. Interestingly, they found that treatment with the tolerizing cytokines TNFα and prostaglandin E2 actually resulted in DCs that were softer than immature cells. Tolerogenic DCs exhibiting partially immature phenotypes have been

shown to induce differentiation of regulatory T-cells [53-55]. This effect is usually attributed to low expression of T-cell ligands or cytokines, but based on our data, we propose that biophysical properties of the DC cortex also play a role. Thus, it will be important going forward to ask how DC stiffness is modulated in response to pro- and anti-inflammatory stimuli, and whether this further shapes T-cell responses.

While the primary focus of this study is on T-cell stiffness responses at the low end of the range (1 – 12 kPa), we noted that very stiff substrates. (25kPa hydrogels and plastic surfaces, which are in the GPa range) elicit strong responses. This was true for proliferation, IL-2 secretion and degranulation. Similarly, recent analysis of human $CD4^+$ effector T-cells shows that re-stimulation on soft surfaces induces upregulation of genes related to cytokine signaling and proliferation, while restimulation on stiff surfaces (100 kPa) triggers expression of an additional genetic program that includes metabolic proteins related to glycolysis and respiratory electron transport [24]. The physiological relevance of these augmented responses is unclear, since T-cells probably never encounter such stiff stimulatory surfaces *in vivo*. Nonetheless, such findings raise important questions about traditional *in vitro* assays of T-cell function, which often utilize glass or plastic stimulatory surfaces.

Two previous studies have addressed the role of substrate stiffness on naïve T-cell activation, but both were conducted using substrates with stiffnesses higher than those we have measured for DCs. Moreover, the results of the two studies were contradictory. Judokusomo et al. [21] stimulated mouse T-cells with acrylamide surfaces ranging from 10-200 kPa. Consistent with our findings, they concluded that stiffer substrates induce more activation. In contrast, O'Connor et al. [22] stimulated human peripheral blood T-cells with PDMS surfaces ranging from 50-10,000 kPa, and found that stiffer substrates diminished T-cell activation. The basis for this difference is unclear due to numerous technical differences. One possibility is that on very stiff surfaces, T cells are driven so strongly that viability decreases. Alternatively, the biophysical properties of blood and tissue-derived lymphocytes may be distinct, as these cells encounter very different mechanical environments. Studies aimed at resolving these questions are underway in our lab.

The observation that T-cells respond to APC stiffness is best understood in the context of evidence that TCR signaling involves force transduction. T-cells exert force on the interacting APC through the TCR complex [3-7], with the amount of force corresponding to APC stiffness [4,5].

Though the details are controversial, there is evidence that force applied on the TCR induces conformational changes that trigger signaling [10-12]. Apart from being a requirement for activation [7,8], force transduction has been shown to promote peptide discrimination by influencing bond lifetimes [9,10]. Importantly, it appears that the TCR's ability to sense stiffness is closely related to its ability to transduce force-dependent signals during T-cell-APC interaction. Indeed, there is evidence that signaling downstream of TCR engagement is increased on stiffer substrates [21] and that the location of early tyrosine phosphorylation events corresponds to sites of maximum traction force [6]. We propose that stiffer substrates allow T-cells to exert more force through TCR interactions, and consequently induce more effective signaling. This accounts for the co-stimulatory property of substrate stiffness on T-cell activation.

We find that both naïve and effector T-cells exhibit stiffness-dependent responses. Since DCs increase their cortical stiffness during maturation, a stiffness dependent mechanism for naïve T-cell priming makes biological sense. Effector T-cells, however, interact with a variety of APCs. In particular, cytotoxic $CD8^+$ T-cells are expected to kill any infected cell throughout the body with no stiffness bias. Nevertheless, we found that degranulation of effector $CD8^+$ T-cells is dependent on substrate stiffness, though the relevant range is higher than that observed for naïve T-cell priming. Similarly, Saitakis et al [24]. have shown that restimulating $CD4^+$ effector T-cells on surfaces of different stiffness induces differential expression of hundreds of genes, as well as a stiffness dependent secretion of INFγ and TNFα [24]. Thus, stiffness sensitivity is a general feature of all T-cells tested. This behavior most likely reflects the fact that mechanosensing is an obligate component of the feedback loop that underlies force-dependent TCR triggering.

MATERIALS AND METHODS

Key Resource Table

Reagent type (species) or	Designation	Source or reference	Identifiers	Additional information
antibody	APC/APC-Cy7 anti-CD4 (rat, clone GK1.5)	Biolegend	Biolegend:100411/10041; RRID:100411/AB_312698	Flow (1:350)
antibody	APC/PE-Cy7 anti-CD8 a (rat, clone 53-6.7)	Biolegend	Biolegend: 00711/100721; RRID:AB_312750/AB_312760	Flow (1:350)
antibody	anti-CD3ε (A. hamster, clone 145-2C11)	BioXCell	BioXcell: BE0001-1; RRID: AB_1107634	0.003 µg/mL - 10 µg/mL
antibody	anti-CD3ε (Armenian hamster, clone PV1)	BioXCell	BioXcell:BE0015-5; RRID:AB_1107628	1 µg/mL - 2 µg/mL
antibody	Anti-CD86 (rat, clone GL-1)	BioXCell	BioXcell: BE0025; RRID: AB_1107678	Stain (1:100)
antibody	APC-Cy7 anti-CD86 (rat, clone GL-1)	BioLegend	BioLegend:105029; RRID:AB_2074993	Flow (1:100)
antibody	PE anti-MHC-II (rat, clone M5/114.15.2)	BioLegend	BioLegend:107607; RRID:AB_313322	Flow (1:100)
antibody	APC anti-CD11c (rat, clone N418)	BioLegend	BioLegend:117309; RRID:AB_313778	Flow (1:100)
antibody	PE-antiCD107a (LAMP-1) (rat, clone 1D4B)	BioLegend	BioLegend:121611; RRID:AB_1732051	2 µg/mL
chemical compound, drug	Cytochalasin-D	EMD Millipore	EMD Millipore: 250255; CAS:22144-77-0	10 µM
chemical compound, drug	Latrunculin-B	EMD Millipore	EMD Millipore: 428020; CAS:76343-94-7	10 µM
chemical compound, drug	(S)-nitro-Blebbistatin	Cayman Chemical	Cayman Chemical:13891; CAS:856925-75-2	50 µM
chemical compound, drug	CK666	EMD Millipore	Millipore: 182515; CAS:442633-00-3	100 µM
chemical compound, drug	Y27632	SIGMA	SIGMA:688000; CAS:146986-50-7	25 µM
chemical compound, drug	SMIFH2	SIGMA	SIGMA:344092; CAS:340316-62-3	10 µM
chemical compound, drug	Escherichia coli 026:B6; LPS	SIGMA	SIGMA:L2762; ECN:297-473-0	200 ng/mL

chemical compound, drug	Collagenase D	SIGMA	SIGMA: COLLD-RO; EC#:3.4.25.3	2 mg/mL
chemical compound, drug	IL-2	NIAID, NIH	N/A	25U;100U
chemical compound, drug	streptavidin-coated polystyrene beads	Spherotech	Spherotech: SVP-60-5	
chemical compound, drug	EZ-link NHS biotin kit	Thermo Fisher Scientific	Thermo Fisher Scientific: 21217	
chemical compound, drug	CFSE	Invitrogen	Invitrogen: C34570	
commercial assay or kit	CF555 Mix-n-Stain	Biotium	Biotium:92234	
commercial assay or kit	MACS pan-dendritic cell isolation kit	Miltenyi Biotec	Miltenyi: 130-100-875	
commercial assay or kit	mouse IL-2 ELISA kit	Invitrogen	Invitrogen: 88-7024-88	
gene (mouse)	*Was*; Wiskott–Aldrich syndrome gene	DOI:10.1084/jem.20091245	MGI:105059; NCBI Gene: 22376	
other	Hydrogel surfaces (96 well plates)	Matrigen	EasyCoat Softwell 96G	Customized plates
other	AFM 1 µM spherical polystyrene probe	Novascan	Novascan: PT.PS	Si_3N_4 cantilever k=0.06 N/m
peptide,	Peptide MHC-II Complex	NIH Tetramer	I-A^b	Sequence:
peptide, recombinant protein	Ovalbumin 323–339; $OVA_{323–339}$	Anaspec	Anaspec: AS-27025; LOT:1755317	Sequence: ISQAVHAAHAEINE
recombinant DNA reagent	pLX301 (plasmid)	Addgene	Addgene: 25895; RRID: Addgene_25895	DOI:10.1038/nmeth.1638
software, algorithm	FlowJo	FlowJo LLC	RRID:SCR_008520	
software, algorithm	NanoScope Analysis	Broker	N/A	
strain, strain background (Mice)	OT-II Transgenic mice / OT-II	Jackson Laboratories	Stock: 004194; RRID:IMSR_JAX:004194	B6.Cg-Tg(TcraTcrb)425Cb
strain, strain background (Mice)	*Was*$^{-/-}$; WASP-,WASp-KO	Jackson Laboratories	Stock: 003292; RRID: IMSR_JAX:003292	129S6/SvEvTac-Was^{tm1Sbs}/J
strain, strain background (Mice)	*Hlcsp1*$^{-/-}$; HS1-KO	David Rawlings, MD.	PMCID: PMC394441	
strain, strain background (Mice)	*Fcsn1-/-*	KOMP Repository, UC	MGI:5605764	Fscn1$^{tm1.1(KOMP)\ Vlcg}$

Inhibitors, reagents and antibodies

Cytochalasin-D and Latrunculin-B were from EMD Millipore, (S)-nitro-Blebbistatin was from Cayman chemical. CK666 was from Calbiochem, and Y27632 and SMIFH2 were from Sigma-Aldrich. I-A^b OVA peptide MHC-II complexes (pMHC) were provided as biotinylated monomers by the NIH tetramer core. Flow cytometry antibodies: rat anti-CD4 APC/APC-Cy7, rat anti-CD8a APC/PE-Cy7, were all from BioLegend. Surface coating antibodies: Armenian hamster anti-CD3ε (clone 2C11), and Armenian hamster anti-CD28 (Clone PV1) were from BioXCell. Anti-CD86 CF555 was made by conjugating purified rat anti-CD86 (BioXCell) with CF555 conjugated dye from Biotium as per the manufacturers protocol.

Mice

All mice were housed in the Children's Hospital of Philadelphia animal facility, according to guidelines put forth by the Institutional Animal Care and Use Committee. C57BL/6 mice (WT) were purchased from Jackson Labs. HS1-KO mice on the C57BL/6 background have been previously described[56] and were a kind gift from doctor David Rawlings at the University of Washington. *Was*$^{-/-}$ mice were purchased from Jackson labs[57] and fully backcrossed to a C57BL/6 background. All mouse strains were used as a source of bone marrow from which to generate BMDCs. Mice bearing a gene trap mutation in the Fscn1 gene (Fscn1$^{tm1(KOMP)Vlcg}$), which abrogates expression of the protein Fascin 1, were generated by the KOMP Repository at UC Davis, using C57BL/6 embryonic stem cells generated by the Texas A&M Institute for Genomic Medicine. Because these mice proved to have an embryonic lethal phenotype, fetal liver chimeras were used as a source of bone marrow precursors. Heterozygous mating was performed, and fetal livers were collected after 15 days of gestation and processed into a single-cell suspension by mashing through a 35-µm filter. Embryos were genotyped at the time of harvest. Cells were resuspended in freezing media (90% FCS, 10% DMSO) and kept at −80 °C until used. Thawed cells were washed, counted, resuspended in sterile PBS and injected i.v. into sublethally irradiated 6-week-old C57BL/6 recipients, 1×10^6 cells per mouse. Chimeras were used as a source for fascin KO bone marrow ~6 weeks after transfer. C57BL/6 mice were also used to prepare WT T-cells. OT-II T-cells were prepared from heterozygous OT-II TCR Tg mice, which express a TCR specific for ovalbumin 323-339 (amino acid sequence ISQAVHAAHAEINEAGR) on I-A^b [58].

Cell culture

Unless otherwise specified, all tissue culture reagents were from Invitrogen/Life Technologies. GM-CSF was produced from the B78H1/GMCSF.1 cell line [59]. HEK-293T cells (ATCC) were cultured in DMEM supplemented with 10% FBS, 100 µg/ml penicillin/streptomycin, 2mM GlutaMAX, 25mM Hepes and 0.1mM NEAA.

Generation of bone marrow derived dendritic cells (BMDCs) was performed using the method of Inaba et al [60]. Briefly, mouse long bones were flushed with cold PBS, the resulting cell solution was passed through a 40 µm strainer, and red blood cells were lysed by ACK lysis. Cells were washed once with RPMI-1640 and then either frozen for later use in RPMI-1640 containing 20% FBS, 10% DMSO, or plated in 10 cm bacterial plates in BMDC culture media (RPMI-1640, 10% FBS, penicillin/streptomycin, GlutaMax and 1% GM-CSF supernatant). For transduction, BMDCs were plated in untreated 6 well plates at $2x10^6$ cells/well in 3 ml of BMDC media. For all preparations, BMDC culture media was added on day 3, and replaced on day 6. On day 7, the cultures contained many aggregates of immature BMDCs loosely attached to firmly adherent macrophages. When necessary, differentiation into $CD11c^+$ DCs (typically 80–90%) was verified on day 7 by flow cytometry. Maturation was induced on days 7 or 8. For this, immature BMDCs were harvested and re-plated in BMDC media supplemented with 200 ng/ml LPS (*Escherichia coli* 026:B6; Sigma-Aldrich) for at least 24h. When necessary, maturation was verified by flow cytometry, with mature BMDCs defined as Live/$CD11c^+$/$CD86^{high}$/MHC-II^{High} cells. To generate splenic DCs, spleens from C57BL/6 mice were cut to smaller pieces and digested with Collagenase D (2 mg/ml, Sigma) For 30 min at 37°C, 5%CO_2. Cells were washed and labeled for separation by negative selection using a MACS pan-dendritic cell isolation kit (Miltenyi Biotec).

Primary mouse T-cells were purified from lymph nodes and spleens by negative selection. Following ACK lysis, cells were incubated with anti-MHC-II (M5/114.15.2) and either anti-$CD8^+$ (2.43) or anti-$CD4^+$ (GK1.5) hybridoma supernatants for 20 min at 4°C to purify $CD4^+$ or $CD8^+$ T-cells respectively. After washing, cells were incubated with anti-rat Ig magnetic beads (Qiagen BioMag), and subjected to magnetic separation. To generate cytotoxic $CD8^+$ T-cells (CTLs), purified murine $CD8^+$ cells were activated on 24-well plates coated with anti-CD3ε and anti-CD28 (2C11 and PV1, 10µg/ml and 2 µg/ml respectively) at $1x10^6$ cells per well. After 24h, cells were removed from activation and mixed at a 1:1 volume ratio with complete T-cell media (DMEM supplemented with penicillin/streptomycin, 10% FBS, GlutaMAX, non-essential amino acids, and 2 µL of 2-ME), containing recombinant IL-2 (obtained through the NIH AIDS Reagent Program,

Division of AIDS, NIAID, NIH from Dr. Maurice Gately, Hoffmann - La Roche Inc [61]), to give a final IL-2 concentration of 100 units/mL. Cells were cultured at 37°C and 10% CO_2, and passaged as needed to be kept at $0.8x10^6$ cells/mL for 7 more days. CTLs were used day 8-9 after activation.

Plasmid construction, viral production, and transduction of DCs:

A constitutively active form of WASp (CA-WASp) was engineered by subcloning WASp cDNA into a pLX301 vector (Addgene), introducing an I294T point mutation [62] by site-directed mutagenesis, and confirming by sequencing. To generate recombinant lentivirus, HEK293T cells were co-transfected using the calcium phosphate method with psPAX2 and pMD2.G, together with the DNA of interest in pLX301. BMDC transduction was carried out on day 2 of culture. Lentiviral supernatants were harvested from HEK-293T cells 40hr post transfection, supplemented with 8 µg/ml Polybrene (Sigma-Aldrich), and used immediately to transduce BMDCs by spin-infection at 1000xG, 37°C for 2hr. After resting the cells for 30 min in a 37°C, 5% CO_2, lentivirus-containing media was replaced with normal BMDC culture media. On day 5 of culture, Puromycin (Sigma-Aldrich) was added to a final concentration of 2 µg/ml to allow selection of transduced BMDCs. Maturation of transduced cells was induced on day 8 by adding 200 ng/ml of LPS in Puromycin free media.

Flow Cytometry

All cells were stained with Live/Dead aqua (ThermoFisher) following labeling with appropriate antibodies in FACS buffer (PBS, 5% FBS, 0.02% NaN_3, and 1 mM EDTA). Flow cytometry was performed using an LSR-II or LSR-Fortessa cytometer (BD) and analyzed using FlowJo software (FlowJo LLC). T-cells were gated based on size, live cells, and expression of CD4 or CD8 (depending on experiment). DCs were incubated for 10 min on ice with the Fc blocking antibody 2.4G2 prior to staining. DCs were gated based on size, live cells, and CD11c expression. Mature DCs were further gated based on high expression of MHC-II, CD86 and CD80.

Preparation of stimulatory beads for "trans" activation assays

Anti-CD3ε and anti-CD28 antibodies were biotinylated using EZ-link sulfo-NHS biotin (ThermoFisher). Streptavidin-coated polystyrene beads 6-8 µm in diameter (Spherotech) were then coated with 3 different concentrations of biotinylated antibody: bead saturation (defined by manufacturer), a ten-fold dilution and a hundred-fold dilution. After coating, beads were washed 3 times by gentle centrifugation and blocked by incubation in full T-cell media.

T-cell activation on stimulatory gel surfaces

Hydrogel surfaces spanning a stiffness range of 1 – 25 kPa were obtained from Matrigen. Hydrogel stiffness was verified by AFM at different locations around the hydrogel surface (Figure 2 - Figure Supplement 1). Surfaces were coated with 100 µL of antibody solution containing anti-CD28 (1 µg/ml, Clone PV1) and varying concentrations of anti-CD3ε (clone 2C11) for 3 hr at room temperature. Primary amines in the antibody form covalent bonds with quinone functional groups within the hydrogels. The gel pore size is on the order of tens of nanometers, such that cells can only interact with antibodies bound at the gel surface.

Plastic control wells were coated either overnight at 4°C or for 3 hr at 37°C. Surfaces were washed 3 times with 200 µL of PBS, and blocked for 10 min with T-cell media containing 10% FBS prior to addition of at least $1.5x10^5$ cells/well. For experiments where exogenous IL-2 was added, cells were plated in media supplemented with IL-2 to a final concentration of 5 or 25 Units. For Trans activation assays with coated beads, T-cells were added to the well 30 min prior to the addition of stimulatory beads. To measure IL-2 secretion, supernatants were harvested 16-18 hr post stimulation, and IL-2 concentration was measured using a mouse IL-2 ELISA kit (Invitrogen). For CFSE dilution assays, purified cells were washed once with PBS and stained for 3 min with 2.5 µM CFSE (ThermoFisher). After quenching the excess CFSE by addition of 1 mL FBS for 30 seconds, cells were washed and plated. Cells were harvested 68-72 hr post stimulation for flow cytometry analysis.

Cytotoxic T-cell degranulation assays

Assays were conducted on day 8 or 9 of culture. $2x10^5$ CTLs were plated onto surfaces coated with various concentrations of anti-CD3ε in the presence of 2 µg/mL PE-conjugated anti-CD107a. After 3 hr of re-stimulation, CD107a labeling was quantified by flow cytometry. Cells were gated based on size, live cells, and expression of $CD8^+$. CD107a mean fluorescence intensity (MFI) was extracted using FlowJo.

T-cell priming assays

Priming assays were carried out in round bottom 96 well plates. $50x10^3$ LPS-matured BMDCs were plated in each well and pulsed with $OVA_{323–339}$ peptide at various concentrations (0.1 – 1 µg/ml). $1.5x10^5$ CFSE stained, OT-II $CD4^+$ T-cells were added to each well and allowed to activate for 68-72 hr. Cells were then harvested and analyzed using flow cytometry.

Atomic force microscopy (AFM)

All experiments were carried out at room temperature using a Bruker Bioscope Catalyst AFM mounted on a Nikon TE200 inverted microscope. Micro-indentation measurements were made with a spherical tip from Novascan. The tip was comprised of a 1 µm silicon dioxide particle mounted on a silicon nitride cantilever with a nominal spring constant of 0.06 N/m; each cantilever was calibrated using the thermal fluctuation method. The AFM was operated in fluid contact mode, at a 2 Hz acquisition frequency. Total vertical cantilever displacement was set to 5 µm, producing a maximal approach/retraction speed of ~20 µm/sec. Maximal deflection (Trigger threshold) was adjusted for each cantilever to apply a maximal force of 6 nN on the measured cell (e.g. for a 0.06 N/m cantilever, the trigger threshold was set to 100 nm). The actual indentation depth was ~1.5 µm depending on the measured cell stiffness (Figure 1 – Supplement Figure 2). Analysis of force-distance curves was carried out using the Nanoscope Analysis software (Bruker). The Young's modulus was extracted using the Hertzian model for spherical tips with a contact point-based fitting on the extend curve data. For each individual cell, two separate measurements were conducted at different locations near, but not directly over, the nucleus. The reported cell stiffness value represents the average between these independent measurements. Note that when measurements of cortical stiffness were made over the nucleus, no significant differences in Young's modulus values were found (not shown). To measure BMDC stiffness, $1x10^5$ cells (untreated or LPS matured) were seeded onto a Poly L-lysine coated surfaces (coverslips or hydrogels) and allowed to spread for 4 hr at 37°C, 5% CO_2. Prior to data acquisition, cells were incubated for 10 min with the Fc blocking antibody 2.4G2, washed and stained for CD86 for 20 min, then washed and mounted on the AFM. All antibody incubations and data acquisition steps were performed in L-15 media (Gibco) supplemented with 2mg/ml glucose. For treated cell measurements, drugs [Latrunculin-B (10 µM), Cytochalasin-D (10 µM), s-nitro-Blebbistatin (50 µM), Y27632 (25 µM), CK666 (100 µM), or SMIFH2 (10 µM)] were pre-incubated with the cells at 37°C, 5% CO_2 for 30 min prior to Fc blocking and maintained in the cultures throughout staining and data acquisition.

Statistical Methods

All datasets were subjected to outlier analysis prior to execution of statistical testing. Outliers eleted from the dataset. Testing for a statistically significant difference between experimental groups was done using an unpaired one-way ANOVA test with a post-hoc Tukey correction for multiple comparisons.

Throughout the paper, experiments are biological repeats and not technical replicates. For BMDC assays, a single experiment constitutes measurement of multiple cells from a fresh DC cell culture, starting from frozen or freshly harvested bone marrow. For splenic DCs, a single experiment constitutes measurement of multiple cells freshly purified from the spleen of a single mouse. In each experiment, WT or untreated cells were measured side by side with treated cells as a standard control. For T-cell assays, a single experiment constitutes cells freshly purified from spleen and lymph nodes of a single or multiple mice. All CFSE dilution assays were executed in technical duplicates, although a single data set is presented. When needed, figure legends describe the quantity of technical repeats used in an experiment.

ACKNOWLEDGEMENTS

The authors thank Florin Tuluc and Jennifer Murray from the Children's Hospital of Philadelphia Flow Cytometry core. We thank the biomechanics core of the Institute of Translational Medicine and Therapeutics (ITMAT) at the University of Pennsylvania for use of the Atomic Force Microscope. We thank Dr. Shuixing Li and Dr. Nathan Roy for expert technical assistance, Dr. Nathan Roy and Mr. Tanner Robertson for critical reading of the manuscript, and members of the Burkhardt laboratory for many helpful discussions. This work was supported by NIH grants R01 GM104867 and R21 AI32828 to JKB.

ETHICS STATMENT

All studies, breeding and maintenance of animals was performed under Animal Care and Use Protocol #667, as approved by The Children's Hospital of Philadelphia Institutional Animal Care and Use Committee.

References

1 Dustin, M. L. The immunological synapse. *Cancer Immunol Res* **2**, 1023-1033, doi:10.1158/2326-6066.CIR-14-0161 (2014).

2 Friedl, P., den Boer, A. T. & Gunzer, M. Tuning immune responses: diversity and adaptation of the immunological synapse. *Nat Rev Immunol* **5**, 532-545, doi:10.1038/nri1647 (2005).

3 Hui, K. L., Balagopalan, L., Samelson, L. E. & Upadhyaya, A. Cytoskeletal forces during signaling activation in Jurkat T-cells. *Mol Biol Cell* **26**, 685-695, doi:10.1091/mbc.E14-03-0830 (2015).

4 Husson, J., Chemin, K., Bohineust, A., Hivroz, C. & Henry, N. Force generation upon T cell receptor engagement. *PLoS One* **6**, e19680, doi:10.1371/journal.pone.0019680 (2011).

5 Sawicka, A. *et al.* Micropipette force probe to quantify single-cell force generation: application to T-cell activation. *Mol Biol Cell* **28**, 3229-3239, doi:10.1091/mbc.E17-06-0385 (2017).

6 Bashour, K. T. *et al.* CD28 and CD3 have complementary roles in T-cell traction forces. *Proc Natl Acad Sci U S A* **111**, 2241-2246, doi:10.1073/pnas.1315606111 (2014).

7 Li, Y. C. *et al.* Cutting Edge: mechanical forces acting on T cells immobilized via the TCR complex can trigger TCR signaling. *J Immunol* **184**, 5959-5963, doi:10.4049/jimmunol.0900775 (2010).

8 Pryshchep, S., Zarnitsyna, V. I., Hong, J., Evavold, B. D. & Zhu, C. Accumulation of serial forces on TCR and CD8 frequently applied by agonist antigenic peptides embedded in MHC molecules triggers calcium in T cells. *J Immunol* **193**, 68-76, doi:10.4049/jimmunol.1303436 (2014).

9 Liu, B., Chen, W., Evavold, B. D. & Zhu, C. Accumulation of dynamic catch bonds between TCR and agonist peptide-MHC triggers T cell signaling. *Cell* **157**, 357-368, doi:10.1016/j.cell.2014.02.053 (2014).

10 Das, D. K. *et al.* Force-dependent transition in the T-cell receptor beta-subunit allosterically regulates peptide discrimination and pMHC bond lifetime. *Proc Natl Acad Sci U S A* **112**, 1517-1522, doi:10.1073/pnas.1424829112 (2015).

11 Kim, S. T. *et al.* The alphabeta T cell receptor is an anisotropic mechanosensor. *J Biol Chem* **284**, 31028-31037, doi:10.1074/jbc.M109.052712 (2009).

12 Hong, J. *et al.* Force-Regulated In Situ TCR-Peptide-Bound MHC Class II Kinetics Determine Functions of CD4+ T Cells. *J Immunol* **195**, 3557-3564, doi:10.4049/jimmunol.1501407 (2015).

13 Byfield, F. J., Reen, R. K., Shentu, T. P., Levitan, I. & Gooch, K. J. Endothelial actin and cell stiffness is modulated by substrate stiffness in 2D and 3D. *J Biomech* **42**, 1114-1119, doi:10.1016/j.jbiomech.2009.02.012 (2009).

14 Discher, D. E., Janmey, P. & Wang, Y.-l. Tissue Cells Feel and Respond to the Stiffness of Their Substrate. *Science* **310**, 1139-1143, doi:10.1126/science.1116995 (2005).

15 Engler, A. J., Sen, S., Sweeney, H. L. & Discher, D. E. Matrix Elasticity Directs Stem Cell Lineage Specification. *Cell* **126**, 677-689, doi:10.1016/j.cell.2006.06.044.

16 Lo, C.-M., Wang, H.-B., Dembo, M. & Wang, Y.-l. Cell Movement Is Guided by the Rigidity of the Substrate. *Biophysical journal* **79**, 144-152, doi:10.1016/S0006-3495(00)76279-5.

17 Oakes, P. W. *et al.* Neutrophil morphology and migration are affected by substrate elasticity. *Blood* **114**, 1387-1395, doi:10.1182/blood-2008-11-191445 (2009).

18 Pelham, R. J. & Wang, Y.-l. Cell locomotion and focal adhesions are regulated by substrate flexibility. *Proceedings of the National Academy of Sciences* **94**, 13661-13665 (1997).

19 Solon, J., Levental, I., Sengupta, K., Georges, P. C. & Janmey, P. A. Fibroblast Adaptation and Stiffness Matching to Soft Elastic Substrates. *Biophysical journal* **93**, 4453-4461, doi:10.1529/biophysj.106.101386.

20 Trappmann, B. *et al.* Extracellular-matrix tethering regulates stem-cell fate. *Nature Materials* **11**, 642, doi:10.1038/nmat3339 (2012).

21 Judokusumo, E., Tabdanov, E., Kumari, S., Dustin, M. L. & Kam, L. C. Mechanosensing in T lymphocyte activation. *Biophysical journal* **102**, L5-7, doi:10.1016/j.bpj.2011.12.011 (2012).
22 O'Connor, R. S. *et al.* Substrate rigidity regulates human T cell activation and proliferation. *Journal of Immunology* **189**, 1330-1339, doi:10.4049/jimmunol.1102757 (2012).
23 Basu, R. *et al.* Cytotoxic T Cells Use Mechanical Force to Potentiate Target Cell Killing. *Cell* **165**, 100-110, doi:10.1016/j.cell.2016.01.021 (2016).
24 Saitakis, M. *et al.* Different TCR-induced T lymphocyte responses are potentiated by stiffness with variable sensitivity. *Elife* **6**, doi:10.7554/eLife.23190 (2017).
25 Jung, S. *et al.* In vivo depletion of CD11c+ dendritic cells abrogates priming of CD8+ T cells by exogenous cell-associated antigens. *Immunity* **17**, 211-220 (2002).
26 Mellman, I. & Steinman, R. M. Dendritic cells: specialized and regulated antigen processing machines. *Cell* **106**, 255-258 (2001).
27 Burns, S. *et al.* Maturation of DC is associated with changes in motile characteristics and adherence. *Cell Motil Cytoskeleton* **57**, 118-132, doi:10.1002/cm.10163 (2004).
28 West, M. A., Prescott, A. R., Eskelinen, E. L., Ridley, A. J. & Watts, C. Rac is required for constitutive macropinocytosis by dendritic cells but does not control its downregulation. *Curr Biol* **10**, 839-848 (2000).
29 Garrett, W. S. *et al.* Developmental control of endocytosis in dendritic cells by Cdc42. *Cell* **102**, 325-334 (2000).
30 Comrie, W. A., Li, S., Boyle, S. & Burkhardt, J. K. The dendritic cell cytoskeleton promotes T cell adhesion and activation by constraining ICAM-1 mobility. *J Cell Biol* **208**, 457-473, doi:10.1083/jcb.201406120 (2015).
31 Al-Alwan, M. M., Rowden, G., Lee, T. D. & West, K. A. The dendritic cell cytoskeleton is critical for the formation of the immunological synapse. *J Immunol* **166**, 1452-1456 (2001).
32 Guilliams, M. & Malissen, B. A Death Notice for In-Vitro-Generated GM-CSF Dendritic Cells? *Immunity* **42**, 988-990, doi:10.1016/j.immuni.2015.05.020 (2015).
33 Lutz, M. B., Inaba, K., Schuler, G. & Romani, N. Still Alive and Kicking: In-Vitro-Generated GM-CSF Dendritic Cells! *Immunity* **44**, 1-2, doi:10.1016/j.immuni.2015.12.013 (2016).
34 Na, Y. R., Jung, D., Gu, G. J. & Seok, S. H. GM-CSF Grown Bone Marrow Derived Cells Are Composed of Phenotypically Different Dendritic Cells and Macrophages. *Mol Cells* **39**, 734-741, doi:10.14348/molcells.2016.0160 (2016).
35 Tee, S. Y., Fu, J., Chen, C. S. & Janmey, P. A. Cell shape and substrate rigidity both regulate cell stiffness. *Biophys J* **100**, L25-27, doi:10.1016/j.bpj.2010.12.3744 (2011).
36 Harding, F. A., McArthur, J. G., Gross, J. A., Raulet, D. H. & Allison, J. P. CD28-mediated signalling co-stimulates murine T cells and prevents induction of anergy in T-cell clones. *Nature* **356**, 607-609, doi:10.1038/356607a0 (1992).
37 Bashour, K. T. *et al.* Cross talk between CD3 and CD28 is spatially modulated by protein lateral mobility. *Mol Cell Biol* **34**, 955-964, doi:10.1128/MCB.00842-13 (2014).
38 Shen, K., Thomas, V. K., Dustin, M. L. & Kam, L. C. Micropatterning of costimulatory ligands enhances CD4+ T cell function. *Proc Natl Acad Sci U S A* **105**, 7791-7796, doi:10.1073/pnas.0710295105 (2008).
39 Yamashiro, S. Functions of fascin in dendritic cells. *Critical reviews in immunology* **32**, 11-21 (2012).
40 van Helden, S. F. *et al.* PGE2-mediated podosome loss in dendritic cells is dependent on actomyosin contraction downstream of the RhoA-Rho-kinase axis. *J Cell Sci* **121**, 1096-1106, doi:10.1242/jcs.020289 (2008).
41 Burns, S., Thrasher, A. J., Blundell, M. P., Machesky, L. & Jones, G. E. Configuration of human dendritic cell cytoskeleton by Rho GTPases, the WAS protein, and differentiation. *Blood* **98**, 1142-1149 (2001).

42 Demoulin, D., Carlier, M. F., Bibette, J. & Baudry, J. Power transduction of actin filaments ratcheting in vitro against a load. *Proc Natl Acad Sci U S A* **111**, 17845-17850, doi:10.1073/pnas.1414184111 (2014).
43 Salbreux, G., Charras, G. & Paluch, E. Actin cortex mechanics and cellular morphogenesis. *Trends Cell Biol* **22**, 536-545, doi:10.1016/j.tcb.2012.07.001 (2012).
44 Huang, Y. *et al.* The actin regulatory protein HS1 is required for antigen uptake and presentation by dendritic cells. *Journal of Immunology* **187**, 5952-5963, doi:10.4049/jimmunol.1100870 (2011).
45 Calle, Y., Chou, H. C., Thrasher, A. J. & Jones, G. E. Wiskott-Aldrich syndrome protein and the cytoskeletal dynamics of dendritic cells. *The Journal of pathology* **204**, 460-469, doi:10.1002/path.1651 (2004).
46 Bouma, G., Burns, S. & Thrasher, A. J. Impaired T-cell priming in vivo resulting from dysfunction of WASp-deficient dendritic cells. *Blood* **110**, 4278-4284, doi:10.1182/blood-2007-06-096875 (2007).
47 Bouma, G. *et al.* Cytoskeletal remodeling mediated by WASp in dendritic cells is necessary for normal immune synapse formation and T-cell priming. *Blood* **118**, 2492-2501, doi:10.1182/blood-2011-03-340265 (2011).
48 Beel, K. *et al.* A LARGE KINDRED WITH X-LINKED NEUTROPENIA WITH AN I294T MUTATION OF THE WISKOTT-ALDRICH SYNDROME GENE. *British journal of haematology* **144**, 120-126, doi:10.1111/j.1365-2141.2008.07416.x (2009).
49 Bufi, N. *et al.* Human Primary Immune Cells Exhibit Distinct Mechanical Properties that Are Modified by Inflammation. *Biophysical journal* **108**, 2181-2190, doi:10.1016/j.bpj.2015.03.047 (2015).
50 Wu, P. H. *et al.* A comparison of methods to assess cell mechanical properties. *Nat Methods* **15**, 491-498, doi:10.1038/s41592-018-0015-1 (2018).
51 Vargas, P. *et al.* Innate control of actin nucleation determines two distinct migration behaviours in dendritic cells. *Nat Cell Biol* **18**, 43-53, doi:10.1038/ncb3284 (2016).
52 Renkawitz, J. *et al.* Adaptive force transmission in amoeboid cell migration. *Nat Cell Biol* **11**, 1438-1443, doi:10.1038/ncb1992 (2009).
53 Gordon, J. R., Ma, Y., Churchman, L., Gordon, S. A. & Dawicki, W. Regulatory dendritic cells for immunotherapy in immunologic diseases. *Front Immunol* **5**, 7, doi:10.3389/fimmu.2014.00007 (2014).
54 Doan, T., McNally, A., Thomas, R. & Steptoe, R. J. Steady-state dendritic cells continuously inactivate T cells that escape thymic negative selection. *Immunol Cell Biol* **87**, 615-622, doi:10.1038/icb.2009.46 (2009).
55 Gleisner, M. A., Rosemblatt, M., Fierro, J. A. & Bono, M. R. Delivery of alloantigens via apoptotic cells generates dendritic cells with an immature tolerogenic phenotype. *Transplant Proc* **43**, 2325-2333, doi:10.1016/j.transproceed.2011.06.007 (2011).
56 Taniuchi, I. *et al.* Antigen-receptor induced clonal expansion and deletion of lymphocytes are impaired in mice lacking HS1 protein, a substrate of the antigen-receptor-coupled tyrosine kinases. *EMBO J* **14**, 3664-3678 (1995).
57 Snapper, S. B. *et al.* Wiskott-Aldrich syndrome protein-deficient mice reveal a role for WASP in T but not B cell activation. *Immunity* **9**, 81-91 (1998).
58 Barnden, M. J., Allison, J., Heath, W. R. & Carbone, F. R. Defective TCR expression in transgenic mice constructed using cDNA-based alpha- and beta-chain genes under the control of heterologous regulatory elements. *Immunol Cell Biol* **76**, 34-40, doi:10.1046/j.1440-1711.1998.00709.x (1998).

59 Levitsky, H. I. *et al.* Immunization with granulocyte-macrophage colony-stimulating factor-transduced, but not B7-1-transduced, lymphoma cells primes idiotype-specific T cells and generates potent systemic antitumor immunity. *J Immunol* **156**, 3858-3865 (1996).
60 Inaba, K. *et al.* Generation of large numbers of dendritic cells from mouse bone marrow cultures supplemented with granulocyte/macrophage colony-stimulating factor. *The Journal of Experimental Medicine* **176**, 1693-1702, doi:10.1084/jem.176.6.1693 (1992).
61 Lahm, H. W. & Stein, S. Characterization of recombinant human interleukin-2 with micromethods. *J Chromatogr* **326**, 357-361 (1985).
62 Westerberg, L. S. *et al.* Activating WASP mutations associated with X-linked neutropenia result in enhanced actin polymerization, altered cytoskeletal responses, and genomic instability in lymphocytes. *The Journal of Experimental Medicine* **207**, 1145-1152, doi:10.1084/jem.20091245 (2010).